STM JOURNALS

Journal of
Polymer & Composites

ISSN: 2321-2810 (Online)
ISSN: 2321-8525 (Print)
Volume 11, Special Issue 1, 2023
DOI (Journal): 10.37591/JoPC

http://engineeringjournals.stmjournals.in/index.php/JoPC/index

Review JoPC

A Comprehensive Review of Concrete Containing Magnetically Treated Water

Peddi Shiva Tejaswi[1,*], Chereddy Sonali Sri Durga[2], Chava Venkatesh[2], Bellum Ramamohan Reddy[3], Indukuri Chandra Sekar Reddy[4], T. Muralidhara Rao[5], B. Nagamalleswara Rao[5], Ramavath Charandeepneelesh[1]

Abstract

In Present scenario, Construction has benefited greatly from the characteristics of concrete and the magnetism of water. The procedure of permitting water to pass through the magnetic field is part of creating magnetised water, utilizing those properties of concrete that can affect such as compressive strength, workability, porosity, permeability, durability, water absorption capacity, hydration rate and aqueous ratio. Reduced cement usage and improved mechanical and technical qualities of concrete are the primary goals of switching from conventional water use to magnetic water. The addition of additives to concrete such as super plasticizers (SP), silica fume, natural zeolite steel fibres, Egyptian alumina, steel chips, silica fume, fly ash, pozzolanic materials, and blast furnace slag will increase concrete properties and effective for construction.

Keywords: Magnetizing, concrete, strength, additives, microstructure, effective, construction.

INTRODUCTION

Researchers have become more interested in studying the use of the magnetic phenomena in engineering applications in recent years [1–15]. Modern production requires present day and non-conventional strategies to provide superior constructing materials. A water molecule is typically interested in hydrogen bonding and creating clusters.

***Author for Correspondence**
Peddi Shiva Tejaswi
E-mail: tejaswipeddi.cvr@gmail.com

[1]M. Tech, Department of Civil Engineering, CVR College of Engineering, Vastunagar, Ibrahimpatnam, Telangana, India
[2]Assistant Professor, Department of Civil Engineering, CVR College of Engineering, Vastunagar, Ibrahimpatnam, Telangana, India
[3]Associate Professor, Department of Civil Engineering, Aditya Engineering College, Surampalem, India
[4]Assistant Professor, Department of Civil Engineering, Sree Datta Institute of Engineering and Science, Hyderabad, India
[5]Professor, Department of Civil Engineering, CVR College of Engineering, Vastunagar, Ibrahimpatnam, Telangana, India

Received Date: December 21, 2022
Accepted Date: May 10, 2023
Published Date: June 19, 2023

Citation: Peddi Shiva Tejaswi, Chereddy Sonali Sri Durga, Chava Venkatesh, Bellum Ramamohan Reddy, Indukuri Chandra Sekar Reddy, T. Muralidhara Rao, B. Nagamalleswara Rao, Ramavath Charandeepneelesh. A Comprehensive Review of Concrete Containing Magnetically Treated Water. Journal of Polymer & Composites. 2023; 11(Special Issue 1): S52–S64.

When a magnetic sphere is utilized within the water, the intra-cluster hydrogen connections are weakened, and large scattered clusters form tiny clusters with strong intra-cluster bonds of hydrogen [16–31].

Industrial fibers may be produced using a variety of materials and come in a variety of forms, depending on the intended use.

Numerous industrial applications can benefit from the guided management of reinforcing fibres enhance the mechanical characteristics of cementitious composites, resulting in stronger non-isotropic building materials. The critical issue of maximizing the use of water inside the concrete manufacturing was prompted by the limited supply of tap water. Additionally, concrete's mechanical qualities, notably its workability, compressive strength, splitting strength, and water adsorption, are strongly impacted by the physical and chemical forms of water [32–50].

MAGNETIZED WATER

Process of Magnetizing Water

Development of Electromagnetic Device

Utilizing solenoids with high Dc source currents operating in various ranges, the electromagnetic device was created utilizing the electromagnetic principle. The inner spool's overall diameter was 213 millimeters, while the spool's height was 65 millimeters. A coil of copper-clad wire (14.5 gauge), having a diameter of not less than 2 millimeters (2.94 mm^2 net area of the conductor). The coil's conductor resistance for a meter of wire at 20°C was 2.5 ohms. According to the block design in Figure 1, the internal coil was made up of 1000 copper wire-covered coils that were tightly coiled around a 65 mm hard plastic tube. When direct current flowed through the coil in the processing area, a static magnetic field vertical to the coil was created.

A heavy iron side screen with two screens, one from the top and one from the bottom, each 12 mm thick, deteriorated to form a funnel in order to increase the intensity of the field and concentrate them in the treating space. Six steel rods were used to construct the top, lower and side shields using two reinforcing rings (16 mm diameter). In which the magnetic field lines are focussed, a treatment area that is height of 65 mm and diameter of 65 mm has been created without shielding.

The magnetic field generator, which is shielded on all sides save the core, was created to mimic an MRI scanner. The created magnetic field may be readily changed from 25 to 130 mT by using various DC sources in coil pools. A big variable transformer was employed to create several direct current sources [6].

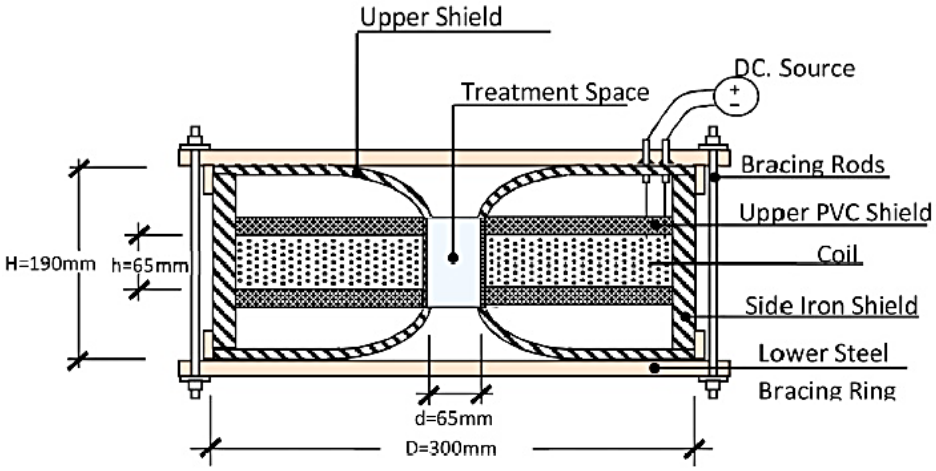

Figure 1. Processing of Magnetized water through electromagnetic device [5].

(a)

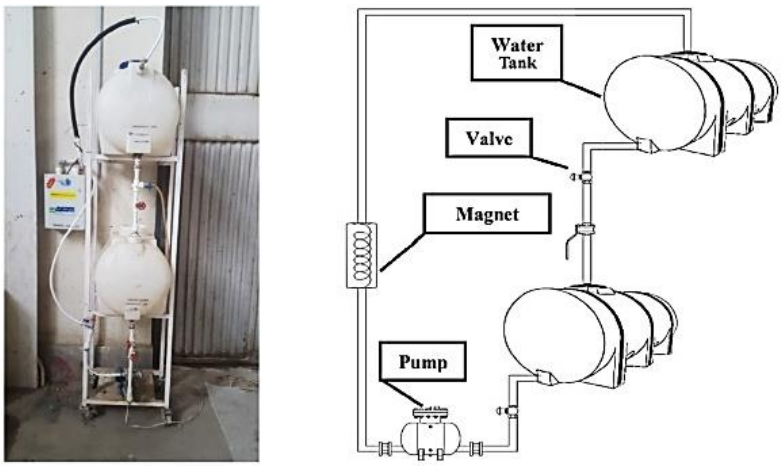

(b)

Figure 2. (a) Process of Magnetizing water [5], (b) Arrangement of water molecules [6].

Physical and Chemical Properties of Magnetized Water

Magnetized water is the result of water passing through the magnetic field. The technique employed and the water's quality regulate the magnetization level [5, 6]. Hydration rates are increased by magnetism because the molecular structures of water are oriented in one specific direction following magnetization and the bond angle changes, resulting in an increase in the viscosity and the surface area, respectively. In research that looked at the impact of a static electromagnetic field on the liquid water. [6] hypothesized that after magnetization, hydrogen bonds were broken, forming stronger hydrogen bonds that resulted in increased viscosity. The arrangement of molecules of water at room temperature is seen in Figure 2(a). When a magnetic field is applied, as illustrated in Figure 2(b), water molecules have a tendency to form hydrogen bound groups, but these groups disintegrate as a result of the magnetic field, enhancing the activities of the water. The water in the layer around the concrete is finer than typical water molecules because the magnetized water molecules are smaller, which results in a lower water need and improves the qualities of the hardened concrete [6].

The Magnetic field strength (MFS) & velocity of water were identified as two influencing elements in the changes brought on by MF [7–8]. Recent years have seen a rise in the usage of Differential Scanning Calorimetry (DSC), one of the most popular techniques for measuring the specific heat of liquids since it can record the heat flow of samples over time and display various thermal behaviors as it heats up [8–10]. At a heating rate of 5 K/min and a gas flow of 13 mL/min for the shielding gas N2, the heat capacity of the tap water and magnetic water samples was determined within 25°C & 70°C. The specimens should be kept at the range for 4 minutes once it has reached 25°C and 70°C. Two empty aluminum containers—a sample container and a reference container—were used for the initial DSC tests [9]. When water and cement are combined, water molecule clusters surround the cement particles. The water layer surrounding the concrete particles are thinner in magnetic water than it is in water from a valve because the clusters are smaller and denser in magnetized water [10].

Figure 3 (a) depicts water molecules as two hydrogen molecules and one oxygen molecule bound in the shape of an isolated triangle with a 105 degrees upper angle. Figure 3 (b) illustrates how the water molecules organize themselves when exposed to a magnetic field.

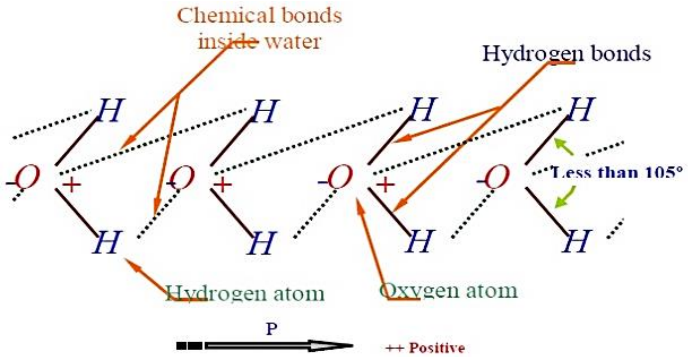

(a)

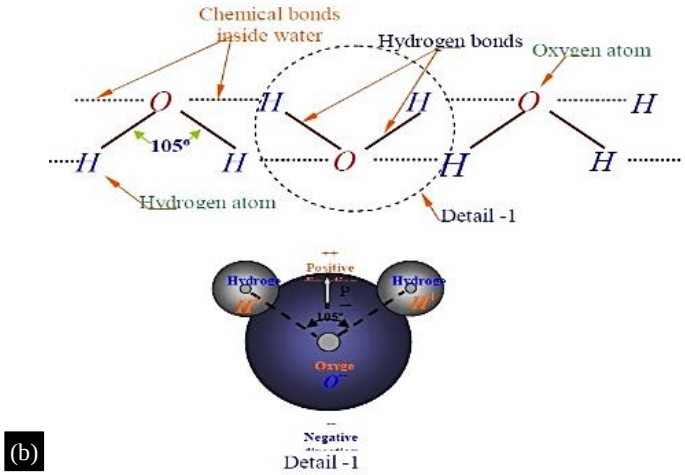

(b)

Figure 3. (a) Molecular arrangement of water molecule, (b) Bond Angle of water molecule [10]

MATERIALS

Steel Fibres

Based on the ASTM C113 standard, Type II Portland cement was employed in this investigation, having a Blaine fitness of 3055 cm^2/g and a density of 3113 kg/m^3 [11]. There were 2600 kg/m^3 density, 6 mm size river sand, and 28% water absorption in the fine aggregate and coarse aggregates chosen according to ASTM C33. Gravel weighing 2613 kg/m^3, 19 millimeters, and one percent was measured in this way: Figure 4(a) displays the fine aggregate and coarse aggregate dimensional categorization curves. The hooked steel fibers, which had lengths of 13 mm and diameters of 0.8 mm, were employed as ferromagnetic fibers, as illustrated in Figure 4(b). Steel fibers had a tensile strength and young's modulus of 913 MPa and 200 GPa respectively [11].

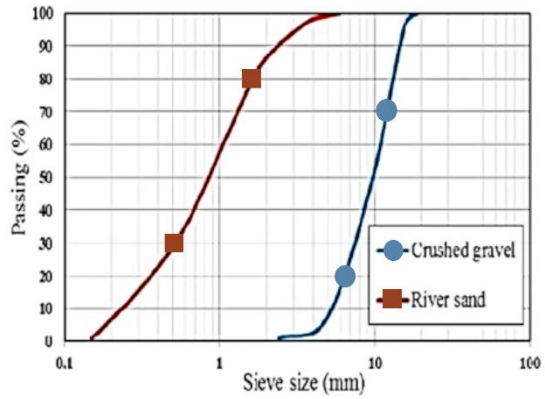

(a)

(b)

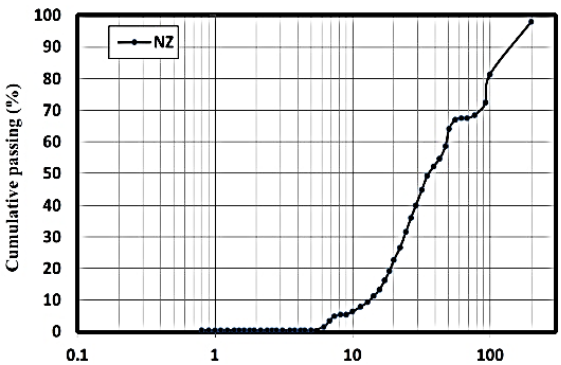

(c)

Figure 4. (a) Dimension curves of fine aggregate and coarse aggregate, (b) Hooked steel Fibers [11], (c) Particle size analysis of NZ [14].

Silica Fume

Silica fume is an extremely fine powder with a spherical shape and a length range of 0.02–1.0 μm. The silica fume utilized in this examination had a specific gravity of 2.2 [12].

Natural Zeolite

The laser diffraction technique was used to analyze the particle size distribution in NZ (Figure 5). The findings indicated that the NZ was between 0.8 and 200 μm, with a 3220 cm^2/g surface area. The present investigation, however, utilized NZ and Type II Portland cements having densities of 2.15 and 3.15 g/cm^3, respectively. Natural river sand, which had a fine aggregate specific gravity of 2.6 g/cm^3, had a 2.38 percent water absorption value. Additionally, crushed gravel with a specific gravity of 2.65 g/cm^3 had a water absorption value and maximum nominal size of 1.01 percent and 19 mm respectively. In contrast to SCC formed from tap water, the field strength of water was calculated to be 0.8 T [13]. EFNARC [16] claims that carboxylate-based HRWR has an ASTM C64 density of 1.15 g/cm^3 [14].

Pozzolanic Materials

This study made use of Type II Portland cement, which has a 3.15 g/cm^3 of specific density. SF, MK, RHA, & FA having densities of 2.32, 2.6, 2.09, and 2.5 g/cm^3 were employed to evaluate the blends' fluidity. These pozzolanic and cementitious materials are depicted in Figure 5(a). Crushed gravel with a specified maximum size of 19 mm made up the coarse aggregate, which had a 2.66 g/cm^3 of specific gravity. In the meanwhile, 2.6 g/cm^3 natural river sand was employed as fine aggregate. The both fine and coarse aggregates had water absorption rates of 2.5% and 1.1%, respectively. Compared to SCC formed from regular water, the mix water utilized for the slurries was 0.8 Tesla magnetic water. EFNARC [15] states that HRWR with a carboxylate base and of density 1.15 g/cm^3 utilized according to ASTM C64 [16].

Steel Chips

Tap water and regular Portland cement were used in all tests. To make the magnetic particles, it has been employed with a 15-aspect ratio jagged steel chips of around 15 mm (0.6 inch) (Figure 5(b)). The river sand used for the aggregates had 2.36 mm (0.09 in) of maximum grain size. As for the PR samples, 3-millimetre-thick plastic moulds were employed to reduce magnetic losses caused by steel mould presence during magnetization [17].

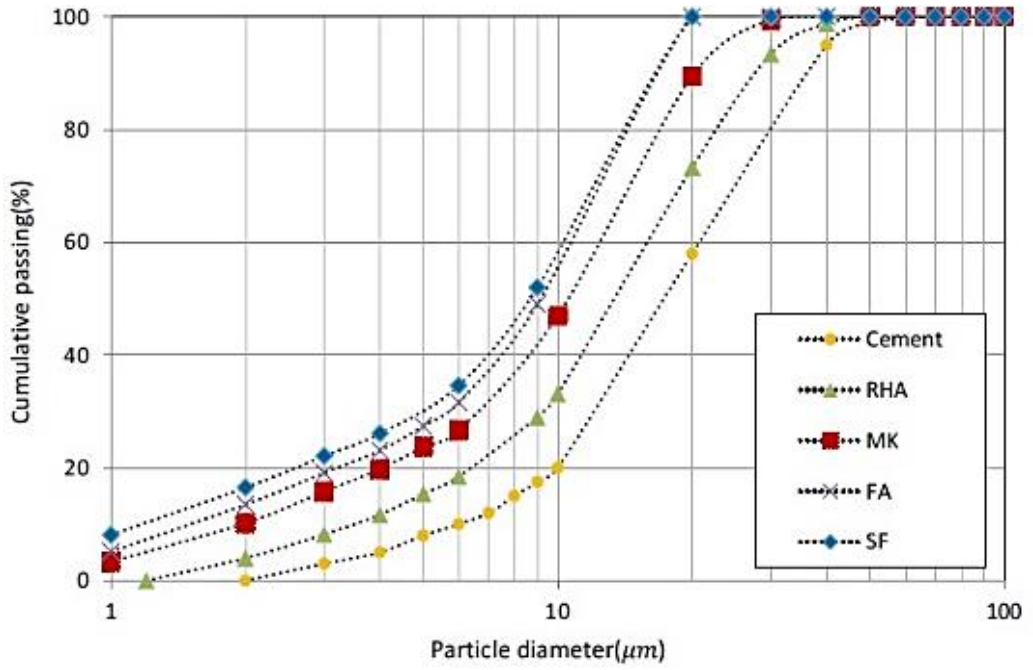

(a)

(b) 

Figure 5. (a) Pozzolanic materials curves for particle size distribution, (b)Jagged Steel Chips [16, 18].

Egyptian Nano Alumina

The materials utilised in this study were ordinary Portland cement (OPC) and Egyptian Nano Al_2O_3, which had a 15 nm of average particle size, a 100 m^2/g of Blaine fineness and 99.3 percent impurities. The usage of natural silica sand that complies with ASTM C33 Crushed stone makes up coarse aggregates (maximum size 19 mm). All mixtures contain a 1.1 relative density polycarboxylate (SP) superplasticizer [19].

Fly Ash

Table 1 provides a list of its physical characteristics. In this investigation, equal amounts of fly ash and cement are mixed instead of the latter. [20].

Blast Furnace Slag

It is made using Taiwan Cement Company's Type I Portland cement. The TsuoShui River in Taiwan provides the native coarse and fine aggregates. Sand from Ottawa with a grain size that complies with ASTM C788 standards is the benchmark for creating mortar sample samples [36–48]. Taiwan Tap Water, located near Touliu, is the source of the mixing water. At a rate of 1313 l/h, water is moved through a magnetic field to magnetize it. From ChungLian, Taiwan, comes the water-cooled GBFS. In this investigation, the mixing method substitutes GBFS for cement.

Table 1. Physical Properties of fly ash [20]

Test Item	Test result	ASTM 618 (F Class)
Soundness (%)	0.021	<0.8
After #325 sieve (%)	13.05	<34
Specific Gravity	2.27	-

MIX PROPORTIONS & SAMPLE TESTING

Steel Fibers

According to ASTM C192, the mixture's design was performed. To prevent magnetic leakage, the pastes had been sculpted in plastic containers. At 20–22 °C for 24 hours, moist sacks were used to cure all concrete samples. They were subsequently freed from the mould and stored in humid settings up until the testing period. This study looked at how long of an exposure to UMF affected the SFRC's mechanical and microstructural characteristics. In this regard, 1, 2, & 3 minutes were chosen as the three varied lengths. Concrete's mechanical resistance when subjected to a magnetic field for two minutes was the subject of previous studies including those by Hajforoush et al. and Abavisani et al. [6, 9]. The exposure lengths of 1, 2, & 3 min were chosen for the analytic needs since, to the authors' knowledge, a longer and a shorter time than the previously indicated time may be relevant in the study process [11].

Silica Fume

workability of 75 mm and 30 MPa compressive cylinder energy were achieved by designing five concrete mixtures with w/c ratio of 0.5, in accordance with the ACI-211 mixes layout technique [9]. Superplasticizer was no longer employed in the combination to examine the full effects of magnetic water [12].

Natural Zeolite

There were two groups, G1 and G2, for the twelve SCC mixes that were evaluated based on their E/B ratios. 400 kg/m^3 was the total weight of the cementitious materials. In order to create the SCC mixes, two of them had magnetic water but no NZ, whereas the other two utilized water from the tap and no NZ (control mix). To achieve Markiv et al passing ability's requirements, we needed a greater HRWR test as the proportion of NZ in the SCC blends grew [14].

Pozzolanic Materials

In all, 10 SCC mixes were made using the W/C ratio of 0.37. Approximately 400 kg/m^3 of cementitious materials were used. There were two SCC mixes that included magnetized and regular water to serve as control mixes for the other nine SCC mixes. To replace SF, MK, RHA, & FA at 10% & 20% of the total cementitious ingredients, eight were combined with magnetic water. The natural aggregates were initially homogenized for 30 seconds at regular mixing speed. One minute of mixing is then completed by adding the mixer with roughly half the water. To allow the aggregates to absorb, the mixture was then let to stand for 1 minute. After another minute of mixing, cement and fillers were added. After 3 minutes of mixing, the dough received the last additions of the remaining water & HRWR. The SCC was produced using the process devised [15]. In accordance with ASTM C66, cylindrical specimens of 15 × 30 cm were cast to determine the 28-day split tensile strength, then 15 cm cubes were made to be machine-tested. In comparison to ASTM C39, compression test results after 7 and 28 days [15]. The ASTM C642 standard's 28-day absorption test was also conducted using cubic samples. The day before the test, all samples were collected after 24 hours and stored in the water polymerization regime [16].

Steel Chips

Compression testing was used to characterize the samples' mechanical properties in accordance with ASTM standard. The PO samples were sandwiched between two cylindrical steel pieces measuring 70 mm (2.76 inches) of diameter to concentrate the magnetic flux across the sample and reduce magnetic loss during testing. These steel pieces were likewise utilised to test the N & PR specimens in order to carry out all the experiments together under the circumstances. The top and lower support blocks of the test machine were in contact with the terminals of the AMF generator to apply AMF. During the test, every PO sample was subjected to AMF until it fell apart [17].

Egyptian Nano Alumina

The cubes utilized for the test of compressive strength have dimensions of 113 × 113 × 113 mm. After being taken out of the mould at one day, all of the samples were kept in the water at 25°C for 28 days. All the cement paste mixtures were manually blended for around five minutes. Then, a sample with a diameter of 13 mm and a thickness of 5 mm was created for microstructure examination (using desorption & SEM approaches). This was followed by 24 hours of curing in a water bath (20 2 degrees C) until the printed samples were old enough to be tested. Each case study had three identical samples for all tests, thus the average of the outcomes was taken into consideration [18–24].

Fly Ash

By combining cementitious materials and ordinary sand in the specified proportions, cubic samples (13 mmx 13 mmx 13 mm) are created. After the samples have hardened for 7, 28, & 56 days at 23 °C and 100 % RH, the mortars compressive strength is assessed [25–37].

Blast Furnace Slag

In accordance with ASTM C109, samples of 5 cubic cm are created by combining standard sand and bonding materials at a weight ratio of 1:2.75. E/B dosages for the blend are 0.4, 0.75, and 0.55 respectively. Water weighs 0.29 times as much as the binder. Compression and hydration tests are performed on 5 cm cubes polymerized at 23°C for seven, 28 & 56 days, respectively, in accordance with the ASTM C109 standard [38–50].

RESULTS AND DISCUSSIONS

Steel Fibers

The experiments clearly showed that the principle of magnetic saturation prevented exposure intervals greater than 3 min from having a substantial impact on the experimental outcomes. 0.7 percent steel fibres were used to achieve the specimens' maximal compressive strength. On concrete cubes measuring 100 mm at 7 and 28 days old, the compression assessment was conducted. Furthermore, a modulus of rupture test in accordance with ASTM C1609 was carried out on 70*70*280 mm prisms at the age of 28. For concrete samples 0.4, 0.7, and 1 percent fractions, respectively, the compressive strength values of the samples rose by 16.42, 20.81, and 16.88 percent after being exposed to ultra-magnetic field for 3 min, volume of steel fibres. Additionally, it may be linked to the increased microstructure density of CSH gel with a higher quantity, which causes a decrease in concrete porosity. As a result, concrete now has much more mechanical strength. This result is somewhat consistent with the findings of Soto Bernal et al. They demonstrated that compared to a plain paste, cement paste with mild magnetic fields (19.07, 22.22, and 25.37 Gauss) had a more compact structures [11].

Silica Fume

In order to measure the concrete's compressive strength (fc') at seven and twenty-eight days, the ASTM C39/C39M compressive strength test was performed, and the cylinders were filled with Sulphur to level the surface. Magnified water and silica fume samples indicate that the mechanical characteristics of concrete may be affected by altering the silica fume level. According to the findings, at a replacement level of 5% for silica fume in magnetized water, the highest compressive strength was 42.72 MPa. The best compressive strength is achieved with an appropriate silica fume replacement level of 10%, according to the literature. Silica fume-rich materials have a greater compressive strength than those that contain no silica fume at all (MS15 and NS15) (MS0 and NS0). To put it another way: When it comes to compressive strength after 28 days of hardened concrete, the situation is inverted, which indicates that specimens containing 0% silica fume have better compressive strength than those with 15% silica fume. In comparison to samples mixed with regular water at the same silica fume level, specimens containing silica fume had a stronger connection [12].

Natural Zeolite

SCC mixes with VSI values ranging around zero and one after mixing were found to be stable, according to EFNARC. The characteristics of cementitious composites are significantly impacted by NZ dispersion. In comparison to the control SCC mix created with magnetic water, it was discovered that the SCC blends including NZ had lower compressive strengths while they were younger. However, as they aged, the opposite was true. According to Ranjbar et al, the explanation is that NZ, which has incredibly small pores and channels, may absorb mixing water. The magnetic water activity in NZ-containing SCC cannot be enhanced over the mixed SCC control at a young age, since NZ has a lower magnetic water activity. Compression strength of the SCC blends having Water to binder ratios of 0.3 and 0.4 was examined at the ages 7, 14, 28, 42 and 90 days, in which the compressive strength was between 22.8 to 58.9 MPa for concrete groups both G1 and G2 and between 25.4 to 13.8 MPa for concrete groups G1. The tensile strengths of concrete from groups G1 and G2 ranged from 2.4 to 4.1 MPa and 2.5 to 3.9 MPa, respectively [14].

Pozzolanic Materials

When comparing to the SCC reference combination prepared with tap water, the strength of concrete for SCC mixes with magnetized water and 20 percent SF, FA, MK, and RHA rose to 6

percent, 33 percent, 26 percent, and 1 percent at the age of 28 days. They came to the conclusion that MK undergoes a pozzolanic reaction to form hydrated calcium silicate and hydrated calcium aluminosilicate hydrates when exposed to excess calcium hydroxide produced by conventional hydration of Portland cement. In order to boost the concrete strength of SCC mixes with binary & ternary mix components, MK developed this new process. Tensile strength for magnetic water and 20% SF, FA, & RHA SCC controls at 28 days of age was greater than that of mixed SCC controls generated with tap water. For SCC having 20% SF, the greatest strength of concrete at 28 days was attained (57 MPa), this could be because other mixes at 28 days of age had larger pozzolanic reactions [15].

According to CEBFIP, water absorption ratings of 5 percent and above, 3 to 5 percent, and 0 to 3 percent were categorized as poor, fair, and good, respectively. In light of this, all concrete mixtures may be categorized as "excellent" and as having "middle-aged" quality. The maximum and lowest values in water absorption were achieved for the SCC reference solution prepared with water from the tap and of SCC with magnetic and SF water, respectively. Water absorption including every mix varied from 1.9 percent to 4.2 percent [16].

Steel Chips

The steel chips vibrated when the PR specimens were subjected to the AMF due to the magnetic field's powerful effects. The average density difference between the N & PO samples and the PR samples was roughly 1.6 percent. The strength of concrete of the initial group was roughly 31.9 percent greater compared to the second group, according to a comparative of the PR d3 specimens with the PR d1 specimens. This means that the compressive strength was greatly impacted by the application of AMF to freshly formed SCRC, leading it to acts like an orthotropic [17].

Egyptian Nano Alumina

All magnetic concrete mixtures have higher slump values than non-magnetic concrete mixtures. A 38, 37, 39 & 38% increase in sag occurs when NA replacement amounts of 0, 1, 2, or 3% are used in the study. When a 1 percent substitution level was used instead of a 0 percent NA mix, the amount of the improvement in compressive strength after 28 days reached roughly 13 percent. Due to the ability of nanoparticles to serve as cementitious phase nuclei, promote cement hydration further due to their high reactivity, and act as a nano reinforcement, densifying the micro-structure as well as the ITZ, which reduces porosity, concrete's compressive strength has increased. In order to improve compressive strength, the nanoparticles would also fill the pores [18–21]. It is clear that if the NA concentration is raised over 1, rather than improving, the composites' compressive strength will rise. When NA substitution levels of 2 percent and 3 percent were used, as opposed to the 0 percent NA mix, the amount of compressive strength loss at 28 days reaches around 8 percent and 25 percent. These results are consistent with those from, whose findings showed that adding 1 percent NA to the mixture significantly increased compressive strength [22–24].

Fly Ash

Concrete made using tap water has a compressive strength that is 0.2–1.35 T less than concrete mixed with Magnetized water concrete. The Magnetic flux density of 0.8 and 1.2 T can also be used to boost compressive strength the most. The compressive strength of all concrete specimens produced using tap water and Magnetized water increases as the cure age increases [25–32]. Concrete samples with 5 percent, 10 percent, and 15 percent fly ash exhibited 4 percent, 14 percent, and 23 percent better compressive strength than those without replacement when the hardening age was prolonged to 90 days [33–35]

Blast Furnace Slag

As the hardening age extends, a rise in compressive strength may be seen. There is a consistent rising trend in the Water to binder ratio of 0.4 samples regardless of the GBFS. In other words, samples combined with magnetic water and tap water, as well as samples with various GBFS levels,

all exhibit a similar pattern of increased resistance [38–44]. The 15 and 25 percent blast furnace slag replacement specimens exhibit an improvement in strength properties of 9 and 4 percent, respectively, after the age was raised to 56 days. It took 28 days and 56 days for the GBFS-containing concrete to show a substantial increase in strength. GBFS and cement hydration product calcium hydroxide have been known to have a long-term pozzolanic reaction. Additionally, this is because the GBFS format employed here has a fineness of 4074 cm^2/g as opposed to concrete particles, which have a fineness of 3054 cm^2/g. The largest gain in compressive strength is attained with a 15 percentage blast furnace slag replacement at 28 and 56 days [45–50].

CONCLUSIONS

A slight increase in density (2% in the concrete mix) was achieved with just a minor increase in compressive and tensile strength (29% and 27%, respectively) while flowability remained constant (25%). To more thoroughly investigate the state of the concrete during the 6-month test, the long-term inquiry was examined. The testing findings unequivocally show that concrete's compressive strength has increased by 3 to 12 percent. With a 12-percent increase in compressive strength, the MTI 400 mT exhibits the finest long-term performance.

The treated mixture is denser and has fewer voids, as demonstrated by a microscopic comparison of the treated and untreated samples. In treated specimens, the cement gel is more vibrant and active, and the dispersion around the filler components is good [5]. Concrete's ability to resist cracking may be considerably increased by using magnetic water. The magnetic field's intensity and length determine the degree of the amplification. Specimens' total fracture area of unit area drops by 72.2% when magnetized at 260 mT with a magnetic flux range of 280 mm. Concrete's rate of shrinkage may be slowed down by using magnetic water; when concrete is combined with tap water, its deformation factor is 140.02, compared to 112.11 for MWCC1 [11].

A three-minute exposure time enhanced the compression strength of the materials to 16.42 percent, 20.81 percent, and 16.88 percent for the mixtures containing 0.4 percent, 0.7 percent, and 1 percent fibre, respectively, steel. Furthermore, after being exposed to UMF for 3 minutes, the SFRC samples' flexural strengths increased by 18.93%, 27.44%, & 26.89%. To improve the mechanical qualities of the concrete, SEM research showed that with extended exposure durations to UMF, the CSH gel shape grew denser and much less porous. With longer UMF exposure times, cement hydration increased [12]. The combinations with 20% FA, 10% FA, and 0% FA had the best cycle counts of 13, 100 & 113 respectively. As a result, the quantity of cycles needed for magnetization increases with decreasing FA concentration. The results of the UPV test were inaccurate and did not accurately depict how MW affected the cement mortar. The usage of MW increases the mortar's usability and, consequently, the flyash by a maximum of 70%. [16].

The outcomes demonstrated that the mineral admixture silica fume concentration has a direct impact on both the strength properties between concrete and steel bar as well as the concrete's compressive strength. Five percent silica fume concentration yields the highest strength properties and bond strength. 15% of the content. Small steel bars are more affected by silica fume because they have a bigger surface area to cover. As a result, the bigger bar's growth force increases when silica fumes are present. In fact, the magnetic water makes the concrete more fluid, which lowers the number of voids in the sample and raises the binding strength [17].

By including magnetic water into the SCC mixture, the HRWR dose can be reduced by 5 percentage. In addition, compared to an SCC combination having only magnetic water and no natural zeolite, the addition of natural zeolite to SCC created with magnetic water would enhance the dose of HRWR, which is essential for the workability of mixes. Strength of concrete of SCC including NZ was shown to be less compared to the mix proportion of SCC manufactured with magnetically treated water at a young age [18–21], but the converse was accurate when they reached an older age, where 20 percent of NZ usage in SCC produced with magnetized water exhibited the excellent mechanical

properties at an age of 90 with 0.37 & 0.5 water to binder ratios. Intriguingly, when SCC integrating NZ grew older, its compressive strength rose more slowly. A superior blend design for technical property compliance than some other concrete mixtures appear to be the SCC made with magnetized water and contains 20 percentage natural zeolite with an 0.37 E/B ratio [22–24].

In comparison to concrete without replacement, mortars containing fly ash have a reduced compressive strength. As fly ash replacement rates rise with age, the decline in compressive strength becomes even more significant. The loss in compressive strength will, however, become less obvious with extended curing age when the same fly ash is applied Concrete's compressive strength increases most effectively between 0.8 and 1.2 T of water's magnetic resistance. Early development is the most critical time for the usage of Magnetically treated water to improve the concrete's compressive strength [25–37]. It is possible to improve the strength of GBFS mortar samples using magnetized water.

The intensity of the magnetic field in the water affects how much the rise is felt. Mortars have an increased compressive strength of 9(+/-)19% when the water is magnetized up to 1.35T. A similar upward trend in compressive strength is observed in mortar specimens produced with magnetized water and a longer hardening age. Concrete that has been replaced with GBFS has greater compressive strength than concrete that has not. Compression strength increases with age, although this becomes more pronounced when the GBFS replace rate has risen. The improvement in strength properties will also become more apparent as a material age with the same addition of GBFS. In mortar made using magnetic water, the W/B ratio also affects the compressive strength [38–45]. The current tendency is comparable to mortar that has been dampened with tap water. The fluidity of new mortar created using magnetized water is superior to that produced with water from the tap, irrespective of the GBFS level. Concrete's compressive strength may rise by 10 to 23% as a result of magnetized water. When the magnetized water reaches 0.8 or 1.2 T, the largest rise is possible. The concrete compressive strength of samples made with magnetic water and tap water increases similarly with drying. Compressive strength of the concrete with and without the partial replacement of 5% GBFS showed no appreciable variation after 7 days. Compressive strength declines as GBFS content rises. The strength of concrete incorporating GBFS, nevertheless, is higher than that of material without GBFS at 28 days and 56 days. At a 15% GBFS level of replacement, the biggest boost is noticeable. Concrete specimens made using magnetic water will be more hydrated than those made with tap water when the mixture has the same proportion [46–50].

REFERENCES

1. Lim SH, Prusty BG, Pearce G, Kelly D, Thomson RS. Study of magnetorheological fluids towards smart energy absorption of composite structures for crashworthiness. Mechanics of Advanced Materials and Structures. 2016 May 3;23(5):538–44.
2. Xu ZD, Shen YP, Guo YQ. Semi-active control of structures incorporated with magnetorheological dampers using neural networks. Smart materials and structures. 2003 Jan 10;12(1):80.
3. Toledo EJ, Ramalho TC, Magriotis ZM. Influence of magnetic field on physical–chemical properties of the liquid water: Insights from experimental and theoretical models. Journal of molecular structure. 2008 Oct 15;888(1–3):409–15.
4. Ahmed SM, Manar DF. Effect of static magnetic field treatment on fresh concrete and water reduction potential. Case Studies in Construction Materials. 2021 Jun 1;14:e00535.
5. Zollo RF. Fiber-reinforced concrete: an overview after 30 years of development. Cement and concrete composites. 1997 Jan 1;19(2):107–22.
6. Hajforoush M, Kheyroddin A, Rezaifar O. Investigation of engineering properties of steel fiber reinforced concrete exposed to homogeneous magnetic field. Construction and Building Materials. 2020 Aug 20;252:119064.
7. Abavisani I, Rezaifar O, Kheyroddin A. Alternating magnetic field effect on fine-aggregate concrete compressive strength. Construction and Building Materials. 2017 Mar 1;134:83–90.

8. Rezaifar O, Abavisani I, Kheyroddin A. Magneto-electric active control of scaled-down reinforced concrete columns. ACI Struct J. 2017 Sep 1;114(5):1351–62.
9. Tarbozagh AS, Rezaifar O, Gholhaki M. Electromagnetism in taking concrete behavior on demand. InStructures 2020 Oct 1 (Vol. 27, pp. 1057–1065). Elsevier.
10. Wang Y, Zhang B, Gong Z, Gao K, Ou Y, Zhang J. The effect of a static magnetic field on the hydrogen bonding in water using frictional experiments. Journal of Molecular Structure. 2013 Nov 25;1052:102–4.
11. Javahershenas F, Gilani MS, Hajforoush M. Effect of magnetic field exposure time on mechanical and microstructure properties of steel fiber-reinforced concrete (SFRC). Journal of Building Engineering. 2021 Mar 1;35:101975.
12. Ghorbani S, Ghorbani S, Tao Z, De Brito J, Tavakkolizadeh M. Effect of magnetized water on foam stability and compressive strength of foam concrete. Construction and Building materials. 2019 Feb 10;197:280–90.
13. No A. Specification for aggregates from natural sources for concrete. Bs. 1992;882(1992):1–4.
14. Olubambi PA, Andrews A, Mothle TS. Strength behavior of magnesia-based refractories after thermal cycling. International Journal of Applied Ceramic Technology. 2014 May;11(3):524–9.
15. Abed JM, Khaleel BA, Aldabagh IS, Sor NH. The effect of recycled plastic waste polyethylene terephthalate (PET) on characteristics of cement mortar. InJournal of Physics: Conference Series 2021 Aug 1 (Vol. 1973, No. 1, p. 012121). IOP Publishing.
16. Ghorbani S, Sharifi S, De Brito J, Ghorbani S, Jalayer MA, Tavakkolizadeh M. Using statistical analysis and laboratory testing to evaluate the effect of magnetized water on the stability of foaming agents and foam concrete. Construction and Building Materials. 2019 May 20;207: 28–40.
17. Puebla K, Arcaute K, Quintana R, Wicker RB. Effects of environmental conditions, aging, and build orientations on the mechanical properties of ASTM type I specimens manufactured via stereolithography. Rapid Prototyping Journal. 2012 Jul 27;18(5):374–88.
18. ASTM C. Standard specification for concrete aggregates. Philadelphia, PA: American Society for Testing and Materials. 2003.
19. Teychenné DC, Franklin RE, Erntroy HC, Marsh BK. Design of normal concrete mixes. London, UK: HM Stationery Office; 1975.
20. Ahmed SM, Manar DF. Effect of static magnetic field treatment on fresh concrete and water reduction potential. Case Studies in Construction Materials. 2021 Jun 1;14:e00535.
21. ASTM International Committee C09 on Concrete and Concrete Aggregates. Standard Test Method for Splitting Tensile Strength of Cylindrical Concrete Specimens1. ASTM international; 2017.
22. Ahmed SM, Manar DF. Effect of static magnetic field treatment on fresh concrete and water reduction potential. Case Studies in Construction Materials. 2021 Jun 1;14:e00535.
23. Ahmed SM, Manar DF. Effect of static magnetic field treatment on fresh concrete and water reduction potential. Case Studies in Construction Materials. 2021 Jun 1;14:e00535.
24. Afshin H, Gholizadeh M, Khorshidi N. Improving mechanical properties of high strength concrete by magnetic water technology. Scientia Iranica. 2010 Feb 1;17(1).
25. Kevern JT, Nowasell QC. Internal curing of pervious concrete using lightweight aggregates. Construction and Building Materials. 2018 Feb 10;161:229–35.
26. American Society for Testing and Materials. Committee C-09 on Concrete and Concrete Aggregates. Standard test method for flexural performance of fiber-reinforced concrete (using beam with third-point loading). ASTM International; 2013.
27. Soto-Bernal JJ, Gonzalez-Mota R, Rosales-Candelas I, Ortiz-Lozano JA. Effects of static magnetic fields on the physical, mechanical, and microstructural properties of cement pastes. Advances in Materials Science and Engineering. 2015 Apr;2015.
28. Yousry OM, Abdallah MA, Ghazy MF, Taman MH, Kaloop MR. A study for improving compressive strength of cementitious mortar utilizing magnetic water. Materials. 2020 Apr 23;13(8):1971.

29. Astm C. 597, Standard test method for pulse velocity through concrete. ASTM International, West Conshohocken, PA. 2009.
30. Bungey JH, Grantham MG. Testing of concrete in structures. Crc Press; 2006 Jan 12.
31. Wei H, Wang Y, Luo J. Influence of magnetic water on early-age shrinkage cracking of concrete. Construction and Building Materials. 2017 Aug 30;147:91–100.
32. ASTM A. 500/A500M-13: Standard Specification for Cold-Formed Welded and Seamless Carbon Steel Structural Tubing in Rounds and Shapes. ASTM: West Conshohocken, PA, USA. 2013.
33. Olhoeft GR, Smith III SS. Automatic processing and modeling of GPR data for pavement thickness and properties. InEighth International Conference on Ground Penetrating Radar 2000 Apr 27 (Vol. 4084, pp. 188–193). SPIE.
34. Brandt AM. Cement-based composites: materials, mechanical properties and performance. CRC Press; 2005 Jun 30.
35. Reddy BS, Ghorpade VG, Rao HS. Influence of magnetic water on strength properties of concrete. Indian journal of science and technology. 2014 Jan 18;7(1):14–8.
36. MAHABOOB S, Afreen MU, Dola Sanjay S, Deshpande AA, Sucharitha D, Fasiuddin M. ISSN-2455–6300 OCTOBER 2018, SPL ISSUE 10.1.
37. Venkatesh C, Sri Rama Chand M, Ruben N, Sonali Sri Durga C. Strength Characteristics of Red Mud and Silica Fume Based Concrete. InSmart Technologies for Sustainable Development 2021 (pp. 387–393). Springer, Singapore.
38. Ruben N, Venkatesh C, Durga CS, Chand MS. Comprehensive study on performance of glass fibers-based concrete. Innovative Infrastructure Solutions. 2021 Jun;6(2):1–1.
39. Durga CS, Ruben N, Chand MS, Indira M, Venkatesh C. Comprehensive microbiological studies on screening bacteria for self-healing concrete. Materialia. 2021 Mar 1;15:101051.
40. Venkatesh C, Sonali Sri Durga C, Durga S, Muralidhararao T. Evaluation of fire impact on structural elements using ANSYS. Journal of Building Pathology and Rehabilitation. 2021 Dec;6(1):1–5.
41. Bellum RR, Venkatesh C, Madduru SR. Influence of red mud on performance enhancement of fly ash-based geopolymer concrete. Innovative Infrastructure Solutions. 2021 Dec;6(4):1–9.
42. Durga, C. S. S., Ruben, N., Chand, M. S. R., & Venkatesh, C. Evaluation of mechanical parameters of bacterial concrete. In Annales de Chimie-Science des: Matériaux. 2019 Dec;43(6):395–399.
43. Anirudh M, Rekha KS, Venkatesh C, Nerella R. Characterization of red mud based cement mortar; mechanical and microstructure studies. Materials Today: Proceedings. 2021 Jan 1;43:1587–91.
44. Venkatesh C, Nerella R, Chand MS. Role of red mud as a cementing material in concrete: A comprehensive study on durability behavior. Innovative Infrastructure Solutions. 2021 Mar;6(1):1–4.
45. Durga CS, Ruben N, Chand MS, Venkatesh C. Performance studies on rate of self healing in bio concrete. Materials Today: Proceedings. 2020 Jan 1;27:158–62.
46. Venkatesh C, Ruben N, Chand MS. Red mud as an additive in concrete: comprehensive characterization. Journal of the Korean Ceramic Society. 2020 May;57(3):281–9.
47. Venkatesh C, Chand MS, Nerella R. A state of the art on red mud as a substitutional cementitious material. InAnnales de Chimie: Science des Materiaux 2019 Apr (Vol. 43, No. 2, pp. 99–106).
48. Venkatesh C, Nerella R, Chand MS. Comparison of mechanical and durability properties of treated and untreated red mud concrete. Materials Today: Proceedings. 2020 Jan 1;27:284–7.
49. Venkatesh C, Mohiddin SK, Ruben N. Corrosion inhibitors behaviour on reinforced concrete—a review. Sustainable Construction and Building Materials. 2019:127–34.
50. Venkatesh C, Nerella R, Chand MS. Experimental investigation of strength, durability, and microstructure of red-mud concrete. Journal of the Korean Ceramic Society. 2020 Mar;57(2): 167–74.

